Analyst

PAPER

View Article Online
View Journal

Cite this: DOI: 10.1039/c5an00085h

On-chip metal/polypyrrole quasi-reference electrodes for robust ISFET operation†

Carlos Duarte-Guevara,[a,b] Vikhram V. Swaminathan,[c,b] Mark Burgess,[d] Bobby Reddy, Jr.,[b] Eric Salm,[b] Yi-Shao Liu,[e] Joaquin Rodriguez-Lopez[d] and Rashid Bashir*[f,b]

To operate an ion-sensitive field-effect transistor (ISFETs) it is necessary to set the electrolyte potential using a reference electrode. Conventional reference electrodes are bulky, fragile, and too big for applications where the electrolyte volume is small. Several researchers have proposed tackling this issue using a solid-state planar micro-reference electrode or a reference field-effect transistor. However, these approaches are limited by poor robustness, high cost, or complex integration with other microfabrication processes. Here we report a simple method to create robust on-chip quasi-reference electrodes by electrodepositing polypyrrole on micro-patterned metal leads. The electrodes were fabricated through the polymerization of pyrrole on patterned metals with a cyclic voltammetry process. Open circuit potential measurements were performed to characterize the polypyrrole electrode performance, demonstrating good stability (±1 mV), low drift (~1 mV h^{-1}), and reduced pH response (5 mV per pH). In addition, the polypyrrole deposition was repeated in microelectrodes made of different metals to test compatibility with standard complementary metal-oxide-semiconductor (CMOS) processes. Our results suggest that nickel, a metal commonly used in semiconductor foundries for silicide formation, is a good candidate to form the polypyrrole quasi-reference electrodes. Finally, the polypyrrole microelectrodes were used to operate foundry fabricated ISFETs. These experiments demonstrated that transistors biased with polypyrrole electrodes have pH sensitivity and resolution comparable to ones that are biased with standard reference electrodes. Therefore, the simple fabrication, high compatibility, and robust electrical performance make polypyrrole an ideal choice for the fabrication of outstanding microreference electrodes that enable robust and sensitive operation of multiple ISFET sensors on a chip.

Received 15th January 2015,
Accepted 31st March 2015

DOI: 10.1039/c5an00085h

www.rsc.org/analyst

1. Introduction

Challenges faced by the healthcare and regulatory industries are driving the development of new miniaturized biological sensors that promise to revolutionize diagnostics and screening methods.[1,2] The demand from these industries for higher quality biosensing with lower costs could be met by creating novel sensing systems with the ideal characteristics of portability, multiplexed analysis, low-cost, and automation.[3,4] At the fore-front of new approaches for biosensing are the field-effect transistor (FET) strategies for label free molecular and chemical detection.[5,6] Applying more than 50 years of development experience in the semiconductor industry to the diagnostics challenges could be the key to reducing the cost and complexity of biological assays while sustaining the required sensitivity and specificity.[7] Several researchers have explored this concept in the last decade improving methods and devices for FET-based biological sensing. Examples include the use of ion-sensitive field-effect transistors (ISFETs) to electrically monitor different biochemical processes,[8,9] modification of nanowire-FETs with capture molecules to detect the charge of a target analyte,[10] commercial use of highly multiplexed ISFET detection systems to perform fast and inexpensive DNA sequencing,[11] and development of theoretical/numerical frameworks for analysis and modeling of the FET structures.[12] The FET-based sensing technologies promise to fundamentally change

[a]Department of Electrical and Computer Engineering, University of Illinois at Urbana-Champaign, 306 N. Wright St., Urbana, IL 61801, USA
[b]Micro and Nanotechnology Lab, University of Illinois at Urbana-Champaign, 208 N. Wright St., Urbana, IL 61801, USA
[c]Department of Mechanical Science and Engineering, University of Illinois at Urbana-Champaign, 1206 W. Green St., Urbana, 61801 IL, USA
[d]Department of Chemistry, University of Illinois at Urbana-Champaign, 505 South Mathews Avenue, Urbana, IL 61801, USA
[e]Taiwan Semiconductor Manufacturing Company, 9 Creation Rd, Hsinchu Science Park, Hsinchu, Taiwan 300-77, R.O.C
[f]Department of Bioengineering, University of Illinois at Urbana-Champaign, 1270 Digital Computer Laboratory, 1304 W. Springfield Ave., Urbana, IL 61801, USA. E-mail: rbashir@illinois.edu; Tel: +1-217-333-3097

†Electronic supplementary information (ESI) available. See DOI: 10.1039/c5an00085h

strategies for detection of biological entities, and create a new generation of biosensing instruments.

One of the key challenges that has prevented the broad incorporation of ISFETs into biosensing systems is the practical limitation of the conventional reference electrode that is required to operate the transistors.[13] Commonly used Ag/AgCl reference electrodes are too big, fragile, and expensive for applications that use small volumes (*e.g.* droplets) or target portable/disposable devices.[14] To replace common reference electrodes, various micro-fabricated electrodes have been reported in the past.[15] For example, a combination of thin-film metal deposition and agar gel saturated with KCl was used to mimic Ag/AgCl electrochemical referencing mechanisms on a miniature solid-state planar electrode.[16,17] Also, platinum has been treated with hydrogen gas, Nafion, and perfluorosulfonic acid polymer, to create reference electrodes for miniaturized electrochemical cells.[18,19] In addition, greater miniaturization has been achieved with microscopic quasi-reference electrodes (a reference that does not have an established potential but varies predictably under certain conditions)[20] that have been fabricated with iridium oxide[21] and with polyvinyl chloride (PVC) as a passivation layer.[22] Despite good reported stability and reliability, these miniaturized reference electrodes are undermined by complex and expensive fabrication protocols that involve several micro-machining steps, complicated chemical processes, the use of expensive precious metals and reagents, or incompatibility with other processes involved in silicon transistor fabrication. Therefore, due to a combination of complexity, cost, and process compatibility issues, it is unlikely that these previous approaches for miniaturization of reference electrodes will be successful alternatives for referencing FET-based biosensors, especially when the transistors are used for screening applications where multiple reactions are performed in a single assay.

In this paper, we report the simple fabrication of stable and pH insensitive on-chip quasi-reference electrodes through the electrodeposition of polypyrrole (PPy) on patterned metals. The PPy coating process involves cyclic voltammetry to polymerize pyrrole on a working metal electrode. The process was originally described by Bard *et al.*, on platinum and stainless steel wires[23] and has been adopted by many others to create quasi-reference electrodes for electrochemical experiments with small or localized volumes such as scanning electrochemical microscopy.[24,25] We used a similar technique to create on-chip quasi-reference electrodes with photolithography patterned metals and evaluated their robustness and pH stability using open circuit potential measurements. Our results indicate that with the on-chip PPy electrodes random potential fluctuations are less than 1 mV, drift is typically between 1 and 2 mV h^{-1}, and potential changes due to pH variations are normally below 5 mV per pH. Other results demonstrate that the PPy deposition process is compatible with CMOS processes, and that operation of ISFETs with on-chip PPy is robust and sensitive. The electrodeposition of PPy was carried out both on precious (platinum, gold, and palladium) and non-precious metal electrodes (iron and nickel), demonstrating that the polymerization can be performed with metals that are currently used in a standard semiconductor foundry. Also, the PPy quasi-reference electrodes were fabricated on foundry ISFET chips and used to bias the transistor fluid-gate during pH sensing experiments. The sensing performance of ISFETs biased with on-chip PPy is similar to that obtained when the transistor is biased with Ag/AgCl. The similar results obtained with these two kinds of electrodes indicate that the high stability and low pH response of the PPy quasi-reference translates to the ISFET system, allowing robust operation of the transistor as pH sensor with a microreference.

2. Experimental section

2.1 Patterning on-chip microelectrodes

Metal microelectrodes are patterned on oxidized silicon wafers and ISFET chips with a standard lift-off process. Positive photoresist SPR 220-4.5 (Microchem, Westborough, MA) is spin coated and UV-patterned on the substrate. Metals are then deposited using an E-beam evaporator (CHA Industries, Freemont, CA) having a 250 Å titanium adhesion layer and 350 Å of the metal selected to form the electrode. After metal evaporation the wafer is immersed in Remover PG (Microchem), sonicated for 15 min, and rinsed with isopropanol and DI water.

2.2 Electrochemical polymerization of polypyrrole on microelectrodes

Partially oxidized PPy has been deposited in the past on platinum and stainless steel wires through a cyclic voltammetry deposition process for the formation of quasi-reference electrodes.[23] This technique is frequently used to form electrodes for scanning electrochemical microscopy assays.[26] We used a similar method to deposit the PPy on patterned metal leads to form on-chip electrodes to bias the electrolyte. Fig. 1(a) shows a schematic of the three-electrode cell for PPy polymerization and deposition in patterned metal microelectrodes. A polydimethylsiloxane (PDMS) well is bonded to the silicon substrate, the on-chip metal is electrically contacted with a micromanipulator probe, a graphite rod is inserted in the solution, and a Ag/AgCl reference electrode (BASi, West Lafayette, IN) is bridged with a pipette tip filled with Agar gel and 0.1 M $NaClO_4$ for minimization of a liquid junction potential between the organic solvent and the aqueous filling solution in the reference electrode. The well is then filled with 400 μL of acetonitrile containing 10 mM pyrrole and 100 mM of tetrabutylammonium hexafluorophosphate (all chemicals from Sigma-Aldrich). Fig. S1† presents a photograph of the electrochemical cell used in the PPy polymerization on the microelectrode.

The three electrodes are connected to a Reference 600™ potentiostat (Gamry Instruments, Warminster, PA) that performs cyclic voltammetry (CV), sweeping the potential from −0.6 to 1.2 V at a 100 mV s^{-1} rate and an initial/final potential of 0.4 V. The CV process is repeated for the desired number of cycles, depositing the polymer on the working electrode. In

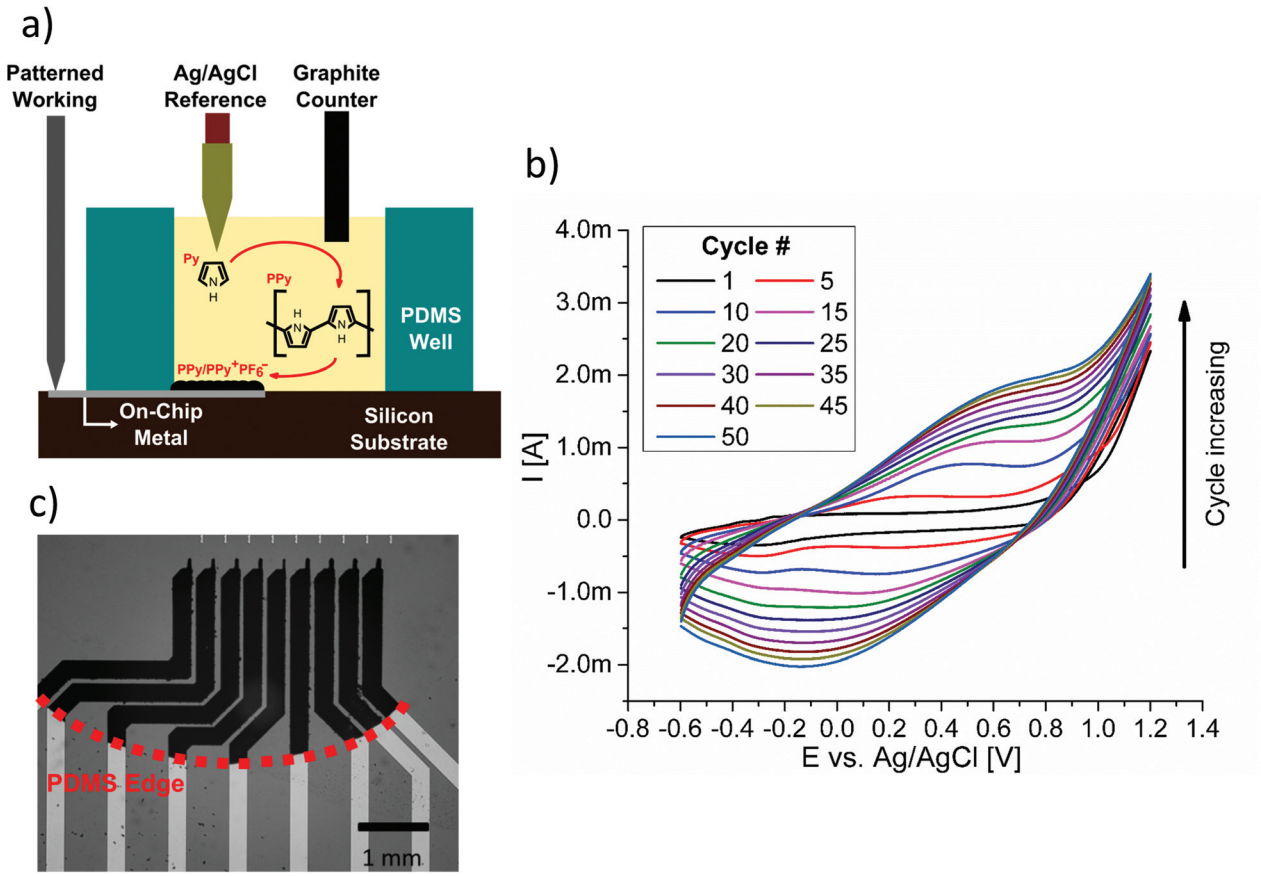

Fig. 1 Electrodeposition of PPy on on-chip patterned metal electrodes. (a) Schematic of the three-electrode cell used for deposition and schematic of the polymerization. The PDMS well is filled with the acetonitrile solution with pyrrole that gets polymerized during CV leaving a film of partially oxidized PPy on the microelectrode. (b) Typical deposition of PPy on platinum microelectrodes by CV, the peak currents increase in each cycle as the PPy electrode grows. (c) Image of independent on-chip platinum electrodes coated with the PPy layer. The edge of the PDMS well is clearly defined owing to the fact that only on-chip metal exposed to the acetonitrile solution is coated.

every iteration, the pyrrole is polymerized and a dark film of partially oxidized polypyrrole ($PPy/PPy^{+}PF^{-}_{6}$) is formed on the exposed microelectrode.

2.3 Physical characterization of film

The polypyrrole film deposited on electrodes was characterized using profilometer and goniometer measurements, optical and SEM imaging, and X-ray diffraction (XRD) analysis. The reported membrane thickness is the total indicator runout (TIR) obtained in a step-high profilometer measurement and the total height of the roughness profile (R_t parameter) is retrieved after applying a 2CR filter to the acquired data. To assess hydrophilicity of the membranes, contact angle measurements were performed on larger electrodes to accommodate 3 μL water droplets. In addition, bright field and SEM images of electrodes were taken with different numbers of PPy coating cycles to evaluate the growth of PPy. The area of the PPy electrode is quantified with ImageJ using the number of dark pixels in the bright field images. Finally, to assess the structural composition of the deposited PPy film, XRD patterns of the electrodeposited polymer were obtained in a continuous scan from 5° to 105° in a PANalytical/Philips X'pert MRD system.

2.4 Open circuit potential measurements

Open circuit potential (OCP) measurements were taken to evaluate stability and response to pH changes of the fabricated microelectrodes. For stability experiments, the PDMS reservoir was filled with a 10 mM KCl solution, the Ag/AgCl (unbridged) electrode was used as the reference, and the on-chip metal was set as the working electrode. The potentiostat was programed to take OCP measurements every half second for one hour after the initial 600 s of stabilization, and each experiment was repeated 3 times. For the pH response analysis, the KCl solution in the PDMS reservoir was spiked with 10 mM HCl or NaOH during the OCP measurement and the pH value was calibrated with an InLab® ultra-micro pH electrode (Mettler-Toledo, Columbus, OH). After the injection, the potential is allowed to stabilize for 600 s and the last 50 s of measurements are averaged to obtain the OCP value for each pH. A pH range of 5.5–8.5 was selected for sensitivity characterization experiments in order to model the behavior of electrodes in regular

physiological buffers and a typical reaction mix of biomolecular assays such as DNA amplification.[22]

The OCP measurements without pH changes are used to quantify stability, repeatability, and drift of the electrodes under evaluation. Stability is the potential variation during a one hour experiment, and is determined by taking the standard deviation of all measurements in an experiment. Repeatability is the variation across the different experiments and is calculated using the average of the standard deviations of measurements in three experiments. The drift measures the changes in potential as a function of time and is the difference of the recorded potentials at the beginning and the end of the experiment. Lastly, the reported pH sensitivity is the absolute value of the slope in a linear regression of the OCP *vs.* pH data.

2.5 ISFET fabrication

ISFET devices were fabricated by Taiwan Semiconductor Manufacturing Company (Hsinchu, Taiwan) with a standard semiconductor process performed on silicon-on-insulator wafers. A complementary metal-oxide-semiconductor (CMOS) process forms the transistor in the device silicon layer. This process is followed by a metallization layer that defines contacts to drain/source nodes and a metallic extended gate that will act as the sensing region. Then, the top inter-layer dielectric is deposited and selectively dry-etched to create openings that reveal the metallic extended gate. The ISFETs are finalized with the deposition of atomic layer deposition (ALD) hafnium oxide over the entire wafer, creating the oxide sensing membrane on top of the extended gate. The use of hafnium oxide as the sensing layer on ISFET pH sensors has been reported in the past. Our group demonstrated that ISFETs made with HfO_2 had a sensitivity of 56 mV per pH, with high linearity, over a range between pH 4 and 10.[27] Other publications have also reported the use of HfO_2 as the sensing layer in ISFETs for larger ranges (pH 2–12),[28] and extended-gate transistors that use high-K dielectrics report high sensitivity and linearity.[29] In Fig. S2† we present pH dependent transistor transfer curves of ISFETs to characterize performance of HfO_2 ISFETs used is this study.

2.6 ISFET testing

To operate ISFETs, source, drain, and gate nodes of the transistors are connected to independent source measure units (SMUs) of a Keithley 4200scs (Keithley, Columbus, OH), and a PDMS well is plasma-bonded to the chip to hold the electrolyte solutions. The transistor fluid gate is swept from −1 to 1 V to obtain transfer characteristic curves that are used to extract threshold voltages using a constant-current extraction method having $I_{th} = 300\ \text{nA}\frac{W}{L}$ where $\frac{W}{L}$ the transistor's aspect ratio.[30] In stability tests, the threshold voltage is measured every minute for an hour to quantify stability and drift. For pH sensitivity experiments, the electrolyte in the PDMS reservoir is titrated with 10 mM NaOH or HCl, and the resulting changes in the threshold voltage are correlated with surface potential to obtain the ISFET pH sensitivity. Testing buffers were selected in the range of pH 6–8 to model the sensor performance in physiological buffers, the master mix of molecular reactions such as PCR or LAMP, or solutions used in protein binding assays.[5]

3. Results and discussion

3.1 Deposition of polypyrrole on microelectrodes

The electrodeposition of PPy in the patterned microelectrodes was carried out in the three-electrode electrochemical cell that is illustrated in Fig. 1(a). Cyclic voltammetry between working and counter electrodes referenced to a bridged Ag/AgCl creates a dark film of partially oxidized PPy in the electrodes that are exposed to the electrolyte. Voltammograms from a typical CV deposition process are presented in Fig. 1(b), which shows the expected shape of CV curves and greater peak/valley currents as the PPy film grows.[23,31] Fig. 1(c) shows PPy-coated platinum microelectrodes on an oxidized wafer. Each electrode was set as the working electrode in independent polymerization, showing that the process is repeatable and will cover the full electrode that is exposed to the acetonitrile solution.

Fig. 2 presents results of PPy film characterization analysis. Profilometer measurements were carried out on electrodes with different deposition cycles to examine the evolution of the PPy film thickness and roughness. Fig. 2(a) shows that the film quickly grows to a few microns in the initial cycles and proceeds to grow linearly in subsequent iterations, reaching around 25 μm at the end of the 50th cycle. A similar trend is observed in the roughness of the growing film. Fig. 2(b) shows that a thicker layer is correlated with a rougher electrode, indicating uneven growth of the PPy layer. In addition, Fig. 2(d) shows that more cycles result in more hydrophilic electrodes. The well-known enhancement relationship between roughness and wettability[32] explains the observed trend of lower contact angles as the hydrophilic PPy layer becomes rougher. The high wettability of the PPy electrodes will simplify their use for applications that use small volumes or droplets. Contact between an on-chip electrode and small volumes can be cumbersome with other approaches that use hydrophobic membranes and therefore would require mechanisms for volume confinement.[33]

Fig. 2(e) and (f) are bright field and SEM images of electrodes with different CV deposition cycles. They reveal the uneven and isotropic growth of the polymer layer. The bright field images show that electrodes with more PPy have a larger area and an irregular shape. Fig. 2(c) presents the quantified relative growth of the electrode area as a function of the number of polymerization cycles. It shows that during the initial cycles the measured area is the same as that of the original electrode indicating that the PPy film grows mostly perpendicular to the silicon. However, in later cycles the PPy layers grow stacked on top of each other resulting in the observed isotropic growth. Fig. 2(f) zooms in on the left portion of the electrode array (for 0, 10, and 50 cycles) and clearly shows that the PPy film becomes thicker and rougher as it grows. The isotropic growth and variability of the deposition process will limit the spatial

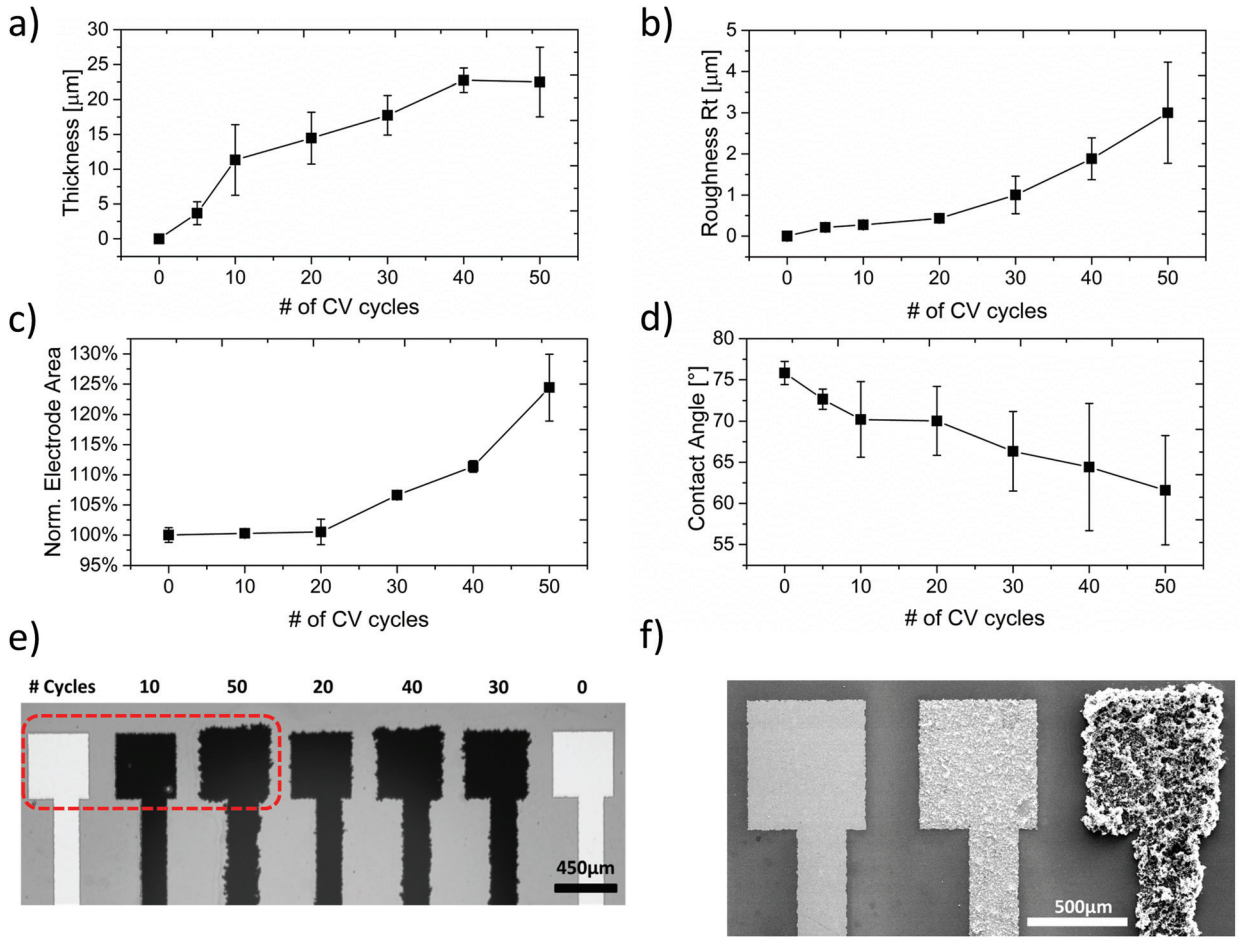

Fig. 2 Characterization of the deposited PPy film. (a) Film thickness, (b) profilometry total roughness (R_t), (c) normalized area of the electrode, and (d) contact angle, as a function of the CV deposition cycles. (e) Optical image of a square electrode array with different numbers of deposition cycles. (f) Scanning electron microscopy image of electrodes in the left side of the array presenting 0, 10, and 50 deposition cycles.

resolution of the PPy electrodes. The horizontal growth of the polymer (parallel to the chip) may cause undesired shorts between patterned electrodes and PPy coating of regions adjacent to electrodes. Therefore, the design of photolithography masks for the lift-off process must take into account this lateral growth and provide adequate spacing between electrodes and on-chip features to prevent shorts or undesired PPy coating during the polymerization. In addition, Fig. S3† shows X-ray diffraction patterns for PPy films deposited on platinum and nickel patterned electrodes. In both cases we observed expected peaks from metal and substrate in addition to peaks at around 24°. These peaks arise from the π-bonds interaction of the PPy chains and it corresponds to a *d* spacing of 0.38.[34] These results indicate that the on-chip electrodeposition yield a normal PPy film that can be used in the electrochemical operation.

3.2 Stability of polypyrrole microelectrodes

The stability of on-chip microelectrodes fabricated with different metals, with and without the PPy film, was quantified with open circuit potential (OCP) measurements against a standard Ag/AgCl reference electrode. For each experiment, OCP measurements were collected for one hour because biochemical reactions that are monitored with ISFETs, such as DNA amplification[35] or protein binding,[36] normally occur within that time frame. Fig. 3(a) shows the measured OCP as a function of time for platinum and gold electrodes with and without PPy. The same figure also shows an OCP stability measurement between two Ag/AgCl electrodes that is used as a benchmark. Data in Fig. 3(a) are presented in the form of "bands" where the thickness is correlated to repeatability of OCP measurements. Each time point for each curve in this plot represents 3 averaged experiments at the same time point with the calculated standard deviation plotted as the error bar. The error bars, which are in close proximity because measurements were taken every half second, create the effect of a thick band. Therefore, the thickness of each band is a representation of the electrode repeatability, and variations in the profile represent the electrode stability. Comparative quantifications of stability and drift are in Fig. 3(b) and (c). The PPy coating makes the electrodes more stable, reducing the variability by around one order of magnitude, and substantially

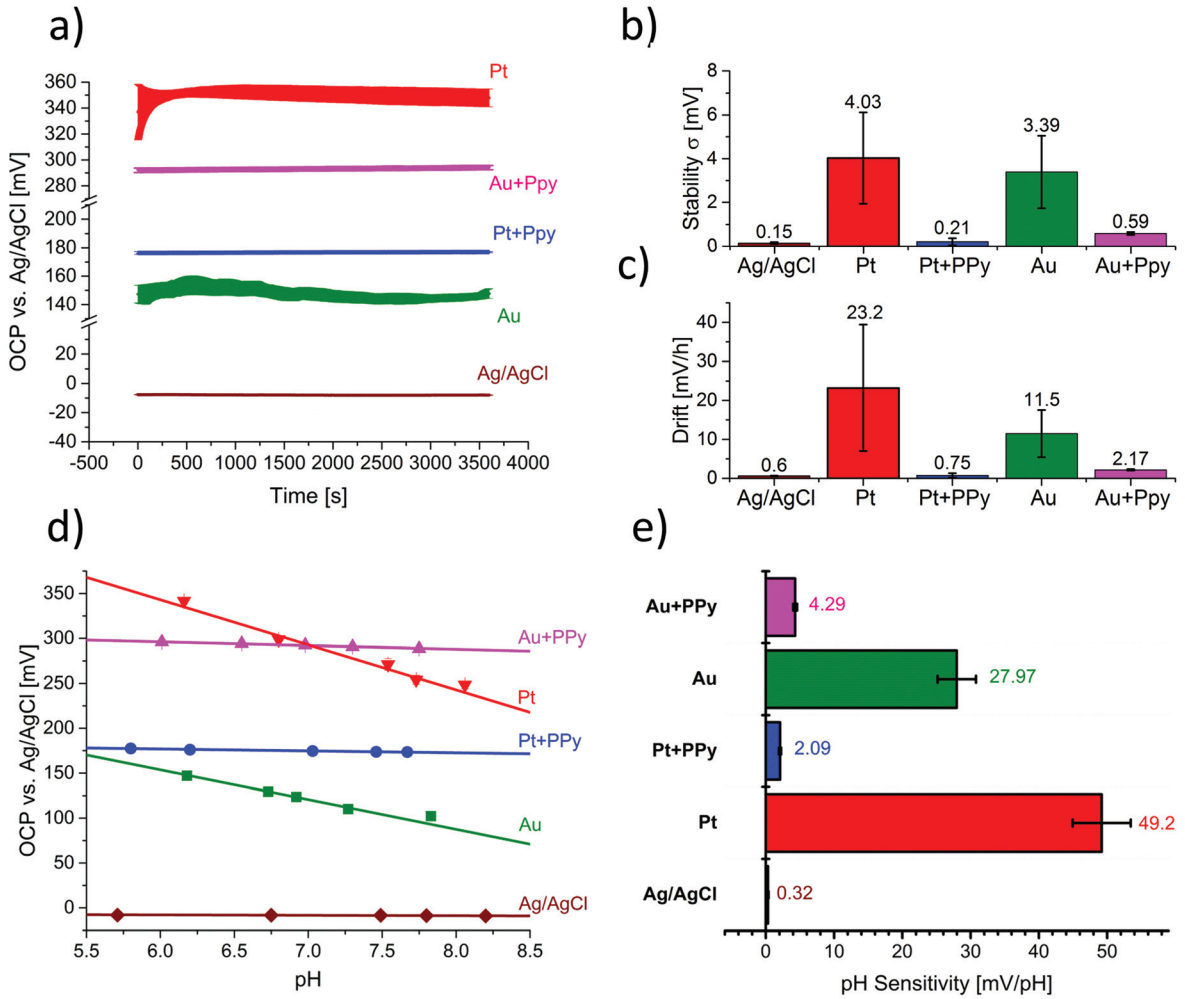

Fig. 3 Open circuit potential (OCP) measurements of electrode stability and pH sensitivity in a 10 mM KCl solution. (a) OCP *vs.* Ag/AgCl as a function of time for each electrode. The bands represent 3 experiments, having the thickness correlated with repeatability, and fluctuations reflecting stability and drift. Comparative quantification of (b) stability and (c) drift of OCP measurements showing improved performance with PPy. (d) Measured OCP as a function of the electrolyte pH with the calculated linear regressions. (e) Extracted pH sensitivity for each electrode demonstrating reduced pH response of the PPy electrodes.

reduce drift. The best results were obtained with PPy coated platinum that has stability and drift comparable to the commercial Ag/AgCl electrode. Although the commercial reference electrode is better than those fabricated with polypyrrole, their stability and possibilities for miniaturization make the PPy electrodes an interesting alternative to the conventional reference electrodes for ISFET operation.

3.3 pH sensitivity of electrodes

Besides providing a stable potential during the experiment, a reference electrode needs to sustain a constant voltage despite changes in the electrolyte.[14] Fig. 3(d) presents the pH sensitivity of gold, platinum, and Ag/AgCl electrodes measured by monitoring the OCP as a function of the electrolyte's pH. Individual plots for each experiment with a different scale that show details of the pH response for each electrode are in the ESI Fig. S4.† The ideal reference electrode response to pH changes is the one observed for the Ag/AgCl reference electrode. With this electrode, despite electrolyte pH variations, the OCP potentials are within 1 mV, resulting in very low pH sensitivity. This is a consequence of the Nernst equation for the Ag/AgCl electrode that is independent of H^+ ions. Experiments with other electrodes show potential variations as a function of pH. The deprotonation and protonation of the electrode's surface is a function of the solution's pH and affects the electrode-localized potential, resulting in pH-dependent OCP.[37] Other publications have reported similar trends and quantification of the sensitivity of metal electrodes to pH changes.[38] However, electrodes coated with the PPy film are substantially less sensitive to pH changes than their bare metal counter parts. The partially oxidized PPy film deposited on the on-chip electrodes is posed by the half reaction $PPy^+A^- + e \rightleftharpoons PPy + A^-$ that allows exchange of ions to sustain a stable potential.[23] The pH titration experiments are summarized in

Fig. 3(e), which compares pH sensitivity of different electrodes. Potentials measured with platinum electrodes are known to have high pH dependence,[22] but after the PPy polymerization the pH sensitivity is reduced by more than 10 times. A similar pH sensitivity reduction is observed for the gold electrode. The PPy layer brings new ion dynamics that result in low pH sensitivities that are significantly smaller than in bare metal electrodes and are required to reference an ISFET.

3.4 Non-precious metal electrodes

Lack of compatibility with semiconductor processes and high manufacturing costs explain why previously reported strategies to create on-chip reference electrodes have not been fully adopted for ISFET operation.[39] The PPy deposition process has been widely reported in gold and platinum wires, but to reduce cost and enable simpler implementation it is necessary to perform the electrodeposition process in non-precious metals. The CV deposition process has been also carried out on a stainless steel wire[23] and others have reported deposition on aluminum at the expense of modifying the electrolyte solution, adding polishing steps, and using electron transfer mediation techniques.[40] To facilitate adaptation of the PPy reference microelectrodes to other standardized fabrication techniques, we attempted the same simple CV PPy deposition process, used in gold and platinum, in metals compatible with CMOS microfabrication steps and evaluated their performance.

The PPy polymerization was also performed on palladium on-chip microelectrodes. Although it is an expensive precious metal, palladium has been used to improve reliability and thermal stability of contact electrodes in MOSFETs and can be incorporated in the CMOS semiconductor processes.[41] The results are presented in Fig. S5,† which shows normal cyclic voltammograms during the deposition process, stable OCP measurements, and a substantial reduction in the pH sensitivity. The next polymerization experiment was performed in iron microelectrodes. The previous polymerization of the PPy layer in steel suggested that iron, which is not currently used for CMOS processes but is an inexpensive commodity material, could be used as a microelectrode in the deposition process. Fig. S6† shows that despite irregular cyclic voltammograms and unexpected reduction of peak currents during the CV process, the deposition of PPy drastically improves stability and pH sensitivity of the electrode. This shows that the PPy coated iron is a stable quasi-reference electrode with performance equivalent to that of the PPy electrodes that use precious metals.

The CV polymerization experiments were also performed with metals that are commonly used in semiconductor foundries. Electrodeposition of PPy on metals that are currently used for metallization layers in the CMOS manufacturing process would strongly facilitate the incorporation of these electrodes in the fabrication process to create on-chip quasi-reference electrodes. In this case, reference electrodes could be easily created in a new metal layer in the surface of the chip that would be coated with PPy using the CV electrodeposition, with no need of additional masks or lithography steps simplifying fabrication. With the same deposition protocol described above we were able to deposit the PPy film on nickel microelectrodes but not on copper, titanium, or aluminum. Although nickel is not used for metal leads in the CMOS process, it is commonly used to create low-resistance nickel-silicide contacts that interface silicon and metal layers in the source and drain nodes.[42] Fig. 4(a) presents the deposition CVs on nickel, showing the expected trend of greater peak currents as the layer grows. These curves also show a secondary process around −0.2 V in reduction. Nevertheless, this process is eliminated in the later cycles, and the final voltammograms are similar to those observed in the deposition on precious metals. Fig. 4(b) presents the stability measurements and Fig. 4(c) shows the pH sensitivity results for both bare nickel and nickel coated with the PPy layer. Once again, quantification of the stability and pH sensitivity demonstrate that the PPy layer significantly reduces potential variations and the response to pH changes of the nickel electrode, demonstrating

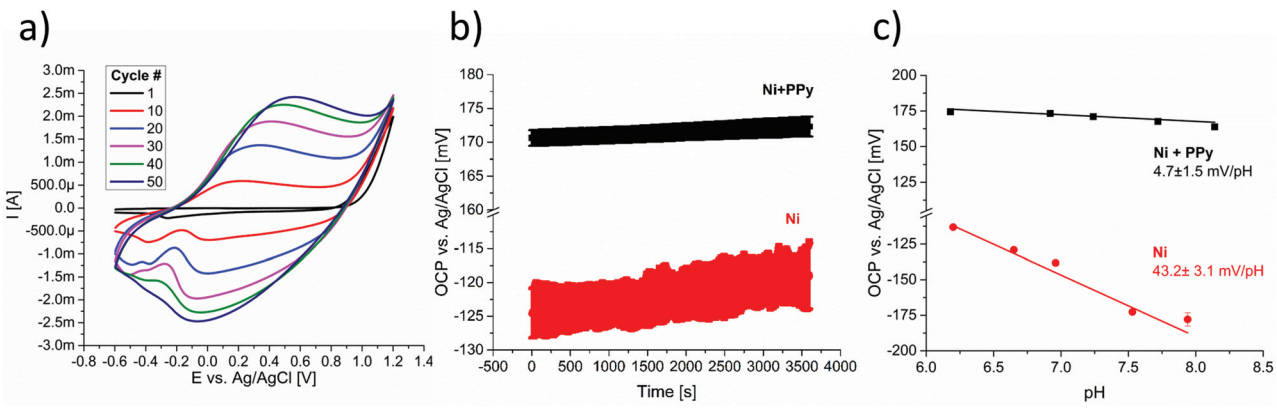

Fig. 4 Polymerization of PPy on nickel electrodes and electrical performance evaluation. (a) CV deposition of PPy film on nickel microelectrodes. (b) Bands of OCP stability as a function of time for nickel with and without the PPy layer. (c) OCP *vs.* electrolyte pH to assess pH sensitivity of nickel and nickel + PPy electrodes. The results of the linear regressions are reported as sensitivity.

Table 1 Summary of stability, repeatability, drift, and pH sensitivity of electrodes made with different metals and with/without the deposited PPy film

Electrode	Stability [mV]	Repeatability [mV]	Drift [mV h^{-1}]	pH sensitivity [mV per pH]
Platinum	4.03 ± 2.09	6.10 ± 1.82	23.2 ± 16.2	49.2 ± 4.25
Platinum + PPy	0.21 ± 0.16	0.67 ± 0.17	0.75 ± 0.53	2.09 ± 0.16
Gold	3.38 ± 1.66	4.42 ± 1.19	11.5 ± 6.07	27.97 ± 2.81
Gold + PPy	0.59 ± 0.06	1.63 ± 0.05	2.17 ± 0.18	4.29 ± 0.28
Palladium	3.32 ± 0.42	10.7 ± 0.42	10.6 ± 0.52	36.2 ± 3.5
Palladium + PPy	0.21 ± 0.12	0.48 ± 0.13	0.92 ± 0.43	8.61 ± 0.57
Nickel	1.72 ± 0.35	3.64 ± 0.4	7.12 ± 1.5	43.19 ± 3.12
Nickel + PPy	0.51 ± 0.10	1.28 ± 0.08	1.73 ± 0.36	4.7 ± 1.56
Iron	6.91 ± 1.11	5.37 ± 2.8	35.8 ± 7.25	29.5 ± 2.03
Iron + PPy	0.44 ± 0.06	1.87 ± 0.05	1.57 ± 0.26	4.71 ± 1.23

that it is possible to create an on-chip quasi-reference electrode with a metal used in a semiconductor foundry.

The electrodeposition of PPy in the other metals typically used in semiconductor foundries suffered from low metal reduction potentials that resulted in the dissolution of the metal thin-film during the CV process or high resistivity of metals and metal oxides that prevented PPy film formation. Previous publications have described other approaches to deposit PPy on these metals.[40,43,44] Nevertheless, those approaches were not pursued because they include additional steps that would complicate the deposition process, undermining desired CMOS compatibility and protocol simplicity. The results of the attempted electrodepositions on copper, aluminum and titanium, including further discussion, are presented in the ESI (Fig. S7–S9†).

Table 1 summarizes the stability and pH sensitivity data for all the electrodes where PPy polymerization was successful, including data for their bare metal counter parts. For all metals, the metal/PPy electrodes presented better stability, improved repeatability, lower drift, and reduced pH response. It is important to note that pH sensing with bare metal electrodes was in general unreliable and only linear in small pH ranges. However, the pH sensitivity evaluation through linear regressions of OCP *vs.* pH data created a standard metric that enabled comparisons between electrodes and demonstrated a clear reduction of the pH sensitivity with PPy electrodes. The main conclusion to be drawn from Table 1 and from the different OCP experiments is that patterned microelectrodes coated with PPy are more stable and less sensitive to pH changes than the metal-only electrodes. Therefore, PPy electrodes are better candidates for on-chip quasi-reference electrodes to operate ISFETs.

3.5 Operation of ISFET with PPy electrodes

Platinum microelectrodes were patterned on an ISFET chip with the lift-off process described previously. The same electrochemical cell used for other PPy depositions on electrodes (Fig. 1(a)) was used for the ISFET chip. A PDMS well is bonded to the top of the silicon die and is filled with the acetonitrile solution. Then, the graphite counter and the bridged Ag/AgCl electrodes are placed inside the well. The deposition cyclic voltammograms are similar to the others reported previously but have lower current peaks because the electrodes on the ISFET chip have a smaller area than the testing structures (Fig. S10†). On the same chip, platinum leads were coated with PPy but others were left exposed for comparative measurements. The result is presented in Fig. 5(a), which shows an extended gate ISFET surrounded by a PPy electrode and an exposed platinum electrode in close proximity.

After the polymerization process, the acetonitrile solution is switched to a 10 mM KCl solution for stability and pH experiments. To modulate drain current, the transistor's fluid-gate is biased with the on-chip electrodes (platinum and PPy) and also with a commercial Ag/AgCl reference electrode. Transfer characteristics of the transistor are presented in Fig. 5(b), where the inset zooms in the region where the threshold voltage is determined. Operation with the 3 electrodes yielded standard transfer characteristics similar to those from other devices with the same fabrication process. The stability of the transistor is evaluated by measuring transfer characteristics every minute for an hour with each electrode in 3 separate experiments. The extracted threshold voltage as a function of time is plotted in Fig. 5(c), along with bars that quantify the threshold voltage drift. As expected, the best stability results are obtained with the commercial Ag/AgCl electrode, the worst with the bare platinum electrode, and intermediate results with the PPy electrode. It is clear that the potential applied to the transistor is more stable and repeatable when the patterned platinum is coated with PPy. Also, the voltage variations and drift are greater in the ISFET experiment than in OCP measurements. This indicates that new noise sources related to the ISFET operation, such as thermal voltage fluctuations or stochastic electrochemical interactions in the gate oxide,[45] harm the transistor's voltage stability.

Evaluation of the ISFET pH sensitivity was performed by measuring threshold voltage variations due to pH changes and correlating them with the change in the oxide surface potential. The same evaluation was performed by biasing the electrolyte with the platinum, PPy, and Ag/AgCl electrodes to compare ISFET pH sensing performance. Fig. 5(d) shows the extracted surface potential as a function of time while the electrolyte pH is changed by titrating NaOH and the full pH-dependent transfer curves are presented in Fig. S11.† Even though there is a clear pH response with the Ag/AgCl and PPy

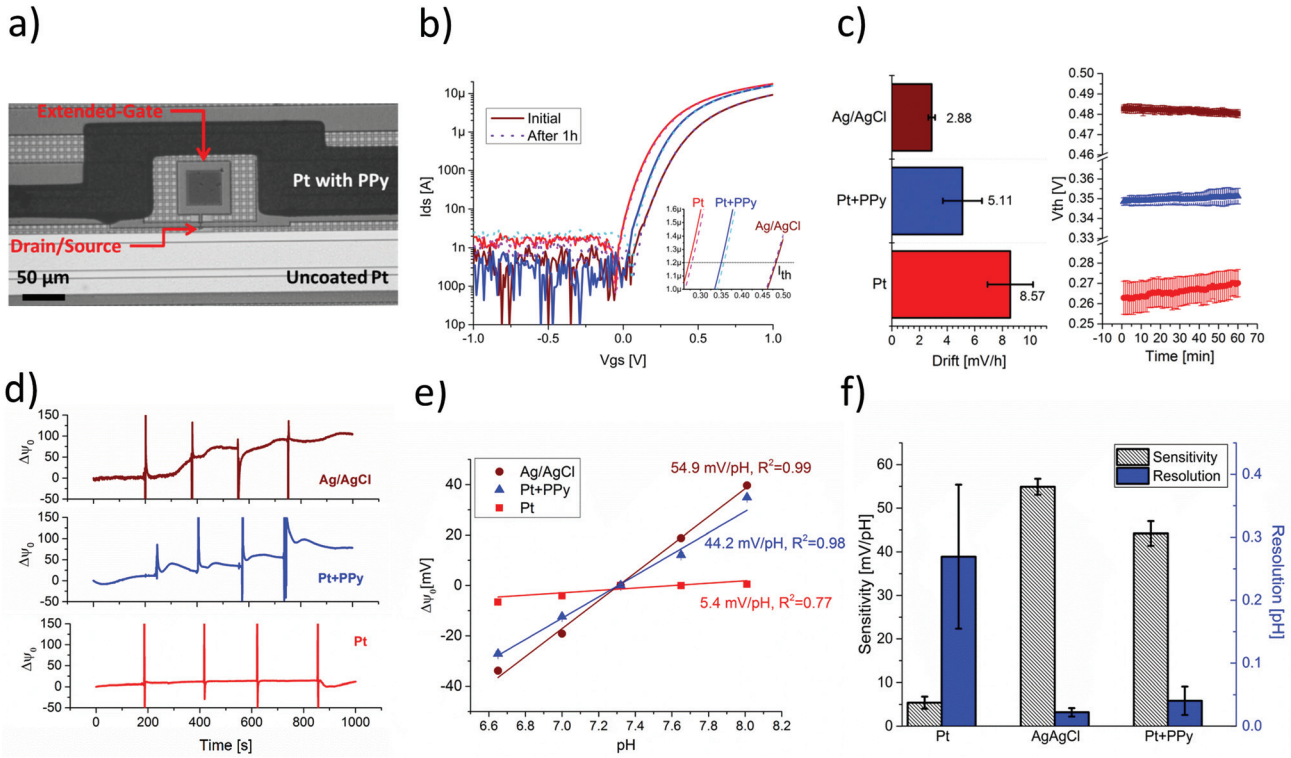

Fig. 5 Evaluation of ISFET operation with PPy microelectrodes. (a) Image of an extended-gate ISFET surrounded by platinum + PPy and bare platinum electrodes used for comparative measurements. (b) ISFET transfer characteristics with platinum, PPy, and Ag/AgCl fluid-biasing electrodes. Solid lines represent the first measurement and dotted lines the last measurement in a one hour experiment. The inset zooms in the area for constant current threshold voltage calculation. (c) Quantification of threshold voltage drift with each electrode and plot of threshold voltage as a function of time during a one hour experiment. Error bars represent variation between different experiments. (d) Real time surface potential variations due to pH changes. The spikes every 200 s in the plot indicate injection of NaOH in the PDMS reservoir and the electrolyte pH-values are the same ones that is plotted in literal 'e'. (e) ISFET surface potential as a function of pH with linear regressions to quantify sensitivity. (f) Comparative results of pH sensitivity and resolution of the ISFET operation with each electrode.

electrodes, the high pH sensitivity of the platinum electrode counteracts the ISFET response, thereby diminishing the recorded surface potential changes in the ISFET. This same behavior has been reported previously and constitutes a strong argument against using platinum electrodes as quasi-reference electrodes for pH monitoring with ISFETs.[22] The quantification of the pH sensitivity is presented in Fig. 5(e), which plots normalized changes in surface potential as a function of the electrolyte pH for the three electrodes. The linear regressions quantify sensitivity and show that the ISFET has sensitivity close to the Nernstian limit when operated with Ag/AgCl, a lower but similar response with the PPy electrode, and very low sensitivity with the platinum electrode. This quantification underscores the importance of minimum pH response of the quasi-reference electrodes. Good ISFET operation is achieved when only the transistor's surface potential changes as a function of the electrolyte pH. Otherwise, other secondary interactions between potentials can undercut pH sensitivity and the ISFET performance. Fig. 5(f) compares the pH sensitivity and resolution of ISFETs biased with the different electrodes. The pH resolution is defined as the ratio of noise to sensitivity ($\Delta pH_{min} = \sigma\psi_s/S$) where $\sigma\psi_s$ is the average of potential fluctuations in each pH measurement (noise), and S is the extracted sensitivity.[35] From this plot we conclude that ISFET pH sensitivity can be greatly improved by coating the microelectrode with the PPy layer. The greater stability and lower dependence of the PPy/electrolyte potential to pH changes result in the ability to sense smaller pH fluctuations (of around 0.04 pH units), which would translate into faster response times and lower detection limits in the biochemical assays. Therefore, the addition of the PPy layer turns patterned microelectrodes into a robust reference for ISFET operation.

A similar pH sensing evaluation was performed for ISFETs operated with nickel-based electrodes. Cyclic voltammograms of the PPy deposition on nickel microelectrodes are presented in Fig. S10† that shows expected shapes but low current. Fig. 6 presents measured sensitivity and stability of an ISFET biased with a Ni + PPy electrode and compares it with results obtained using a bare Ni electrode. Fig. 6(a) shows pH-dependent transfer curves when the ISFET is operated with a Ni + PPy electrode. As shown in Fig. 6(b), the sensitivity quantification yielded a surface potential change of ~39 mV per pH. This is significantly larger than the 15 mV per pH obtained with a bare Ni electrode. In addition, the Ni + PPy electrodes

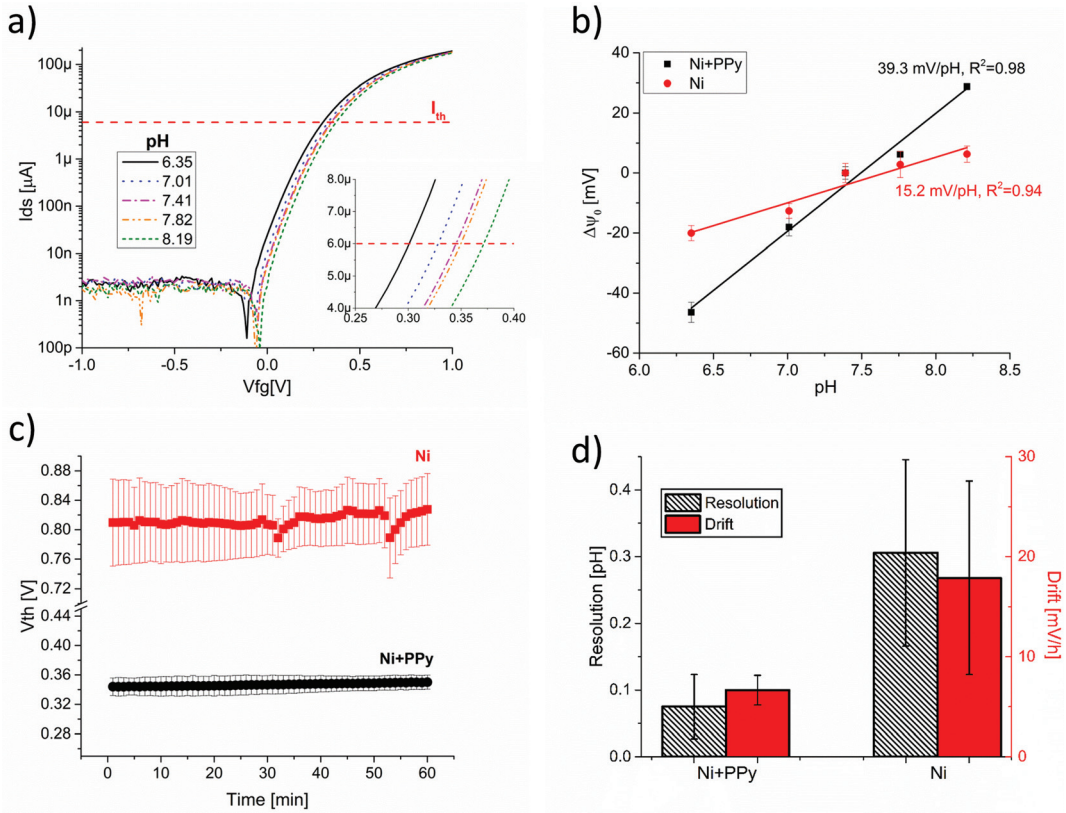

Fig. 6 Assessment of ISFET operation with nickel-based electrodes. (a) pH dependent I_d–V_g transfer curve of ISFET biased with a Ni + PPy electrode. The inset zooms in the area of threshold current that is used to extract change in surface potential. (b) Surface potential variation as a function of pH for transistors biased with bare Ni and Ni + PPy electrodes. (c) ISFET threshold voltage drift with Ni and Ni + PPy electrodes during a one hour experiment. (d) Comparison of pH resolution and threshold voltage drift of ISFETs biased with bare nickel and nickel + PPy electrodes.

are more stable than the bare Ni counterpart. Fig. 6(c) shows the ISFET threshold voltage as a function of time during one hour, demonstrating that measurements performed with Ni + PPy electrodes are more repeatable and have lower noise levels. Comparative measurements of pH resolution and total drift are presented in Fig. 6(d) that summarizes the characteristics of Ni + PPy electrodes. The fine pH resolution and low threshold voltage drift of the ISFET biased with Ni + PPy is consistent with the low pH dependence and high stability observed for coated nickel electrodes in OCP measurements. With both Ni and Pt the electrodeposition of PPy on the patterned electrodes created a robust reference that translates into higher sensitivities and lower noise levels.

The PPy electrodes are well-suited to be efficient on-chip quasi-reference electrodes for ISFET fabrication and operation. The stability and lack of pH response of the PPy electrodes is complemented with a simple and inexpensive manufacturing process. The electrodeposition method has several advantages when compared to other reported alternatives. First, it does not require photolithography and etching steps that are used for other on-chip solid-state reference electrodes. Second, the iteration of CV cycles ensures that all the exposed metal will be covered by the polymer, minimizing performance degradation caused by fabrication defects. Third, unlike other processes that print electrodes, the polymerization of PPy can be easily scaled to create quasi-reference microelectrodes in a parallel deposition process by setting up multiple nodes as the working electrode. In addition, deposition of PPy does not involve chemical surface modifications that may harm the FET's sensing hafnium oxide layer, and the materials required for the process are inexpensive, especially when non-precious metals are used for patterning the microelectrode. These advantages of the PPy electrodes make them good candidates for fabrication of ISFETs with on-chip quasi-reference electrodes.

The PPy electrodes will enable the use of ISFETs to perform and monitor biochemical reactions that take place in small droplets, creating new opportunities for FET-based biological sensing. There are several advantages for performing reactions in small volumes that can be exploited using the microscopic ISFETs. Besides the obvious reduction of reagent consumption, performing reactions in small volumes enables high-throughput screening assays, results in better sensitivity and quantification, and permits fast and low energy thermocycling.[46] Therefore, the robust PPy electrodes solve the issue of droplet electrolyte referencing. They will allow the integration of FETs and droplet reactions creating a path for multiplexed, inexpensive, label-free, and portable biological sensing.

4. Conclusions

In this paper, we presented a robust and low-cost method to create on-chip quasi-reference electrodes for ISFET operation. Simple cyclic voltammetry deposition of polypyrrole on patterned electrodes yielded robust quasi-reference electrodes that have stability and pH response similar to the conventional Ag/AgCl. We characterized the deposited polypyrrole film on the microelectrodes by studying its deposition process and performing open circuit potential measurements to evaluate its electrical performance. We showed the isotropic growth of micrometer polypyrrole layers on the patterned microelectrodes and demonstrated that these quasi-reference electrodes are stable within 1 mV, have a drift of only 1–2 mV h^{-1}, and present a low pH response of around 5 mV per pH. These characteristics are substantially better than the ones obtained with bare metal electrodes and translate into robust ISFET operation with close to Nernstian sensitivity and good pH resolution. Furthermore, we polymerized PPy in different metals demonstrating that the technique can be expanded to non-precious metals like nickel, showing a clear path for integration of these quasi-reference electrodes to the semiconductor foundry fabrication processes.

On-chip reference electrodes are smaller, more robust, less expensive, and simpler to pack than the common glass packed reference electrodes. The polypyrrole on-chip electrodes that we studied have all those desirable characteristics with the added advantages of simple fabrication, low cost, and facile integration with other process of a semiconductor foundry. We believe that these new on-chip electrodes will allow novel applications of ISFET sensing by enabling the use of smaller electrolyte volumes and simplifying implementation of portable applications.

Acknowledgements

We acknowledge funding support from a cooperative agreement with Purdue University and the Agricultural Research Service of the United States Department of Agriculture, project number 1935-42000-035, and a sub-contract to the University of Illinois at Urbana-Champaign. In addition, we acknowledge support from the Center for Innovative Instrumentation Technology (CiiT) of the University of Illinois at Urbana-Champaign.

References

1 J. Lu and M. Bowles, *Qual. Assur. Saf. Crops Foods*, 2014, **6**, 123–133.
2 P. Vadgama, S. Anastasova and A. Spehar-Deleze, in *Detection Challenges in Clinical Diagnostics*, 2013, pp. 35–64.
3 A. J. Baeumner, C. Jones, C. Y. Wong and A. Price, *Anal. Bioanal. Chem.*, 2004, **378**, 1587–1593.
4 P. Yager, G. J. Domingo and J. Gerdes, *Annu. Rev. Biomed. Eng.*, 2008, **10**, 107–144.
5 C. Guiducci and F. M. Spiga, *Nat. Methods*, 2013, **10**, 617–618.
6 G.-J. Zhang and Y. Ning, *Anal. Chim. Acta*, 2012, **749**, 1–15.
7 C. Toumazou and P. Georgiou, *Electron. Lett.*, 2011, 47.
8 D. G. Pijanowska and W. Torbicz, *Sens. Actuators, B*, 1997, **44**, 370–376.
9 A. Soldatkin, J. Montoriol, W. Sant, C. Martelet and N. Jaffrezic-Renault, *Talanta*, 2002, **58**, 351–357.
10 K.-I. Chen, B.-R. Li and Y.-T. Chen, *Nano Today*, 2011, **6**, 131–154.
11 C. Beadling, T. L. Neff, M. C. Heinrich, K. Rhodes, M. Thornton, J. Leamon, M. Andersen and C. L. Corless, *J. Mol. Diagn.*, 2013, **15**, 171–176.
12 K. Lee, P. R. Nair, A. Scott, M. a. Alam and D. B. Janes, *J. Appl. Phys.*, 2009, **105**, 102046.
13 A. Michalska, *Electroanalysis*, 2012, **24**, 1253–1265.
14 I.-Y. Huang and R.-S. Huang, *Thin Solid Films*, 2002, **406**, 255–261.
15 M. W. Shinwari, D. Zhitomirsky, I. a. Deen, P. R. Selvaganapathy, M. J. Deen and D. Landheer, *Sensors.*, 2010, **10**, 1679–1715.
16 I.-Y. Huang, S.-H. Wang, C.-C. Chu and C.-T. Chiu, *J. Micro/Nanolithogr., MEMS, MOEMS*, 2009, **8**, 033050.
17 B. J. Polk, A. Stelzenmuller, G. Mijares, W. MacCrehan and M. Gaitan, *Sens. Actuators, B*, 2006, **114**, 239–247.
18 E. S. McLamore, J. Shi, D. Jaroch, J. C. Claussen, a. Uchida, Y. Jiang, W. Zhang, S. S. Donkin, M. K. Banks, K. K. Buhman, D. Teegarden, J. L. Rickus and D. M. Porterfield, *Biosens. Bioelectron.*, 2011, **26**, 2237–2245.
19 J. Noh, S. Park, H. Boo, H. C. Kim and T. D. Chung, *Lab Chip*, 2011, **11**, 664–671.
20 G. Inzelt, in *Handbook of Reference Electrodes*, ed. G. Inzelt, A. Lewenstam and F. Scholz, Springer Berlin Heidelberg, Berlin, Heidelberg, 2013, pp. 331–332.
21 H. Yang, S. K. Kang, C. A. Choi, H. Kim, D.-H. Shin, Y. S. Kim and Y. T. Kim, *Lab Chip*, 2004, **4**, 42–46.
22 E. Salm, Y. Zhong, B. Reddy Jr., C. Duarte-Guevara, V. Swaminathan, Y.-S. Liu and R. Bashir, *Anal. Chem.*, 2014, **86**, 6968–6975.
23 J. Ghilane, P. Hapiot and A. J. Bard, *Anal. Chem.*, 2006, **78**, 6868–6872.
24 Y. Yoshida, S. Yamaguchi and K. Maeda, *Anal. Sci.*, 2010, **26**, 137–139.
25 D. Zhan, F. F. Fan and A. J. Bard, *Proc. Natl. Acad. Sci. U. S. A.*, 2008, **105**, 12118–12122.
26 L. E. Barrosse-Antle, a. M. Bond, R. G. Compton, a. M. O'Mahony, E. I. Rogers and D. S. Silvester, *Chem. – Asian J.*, 2010, **5**, 202–230.
27 B. R. Dorvel, B. Reddy, J. Go, C. Duarte Guevara, E. Salm, M. A. Alam and R. Bashir, *ACS Nano*, 2012, **6**, 6150–6164.
28 C.-S. Lai, C.-M. Yang and T.-F. Lu, *Electrochem. Solid-State Lett.*, 2006, **9**, G90.
29 K. A. Yusof, S. H. Herman and W. F. H. Abdullah, in IEEE International Conference on Semiconductor Electronics (ICSE), 2014, pp. 491–494.

30 A. Ortiz-Conde, F. J. García Sánchez, J. J. Liou, A. Cerdeira, M. Estrada and Y. Yue, *Microelectron. Reliab.*, 2002, **42**, 583–596.
31 M. Zhou, M. Pagels, B. Geschke and J. Heinze, *J. Phys. Chem. B*, 2002, **106**, 10065–10073.
32 D. Quéré, *Annu. Rev. Mater. Res.*, 2008, **38**, 71–99.
33 H. Suzuki, H. Ozawa, S. Sasaki and I. Karube, *Sens. Actuators, B*, 1998, **53**, 140–146.
34 Y. Ma, S. Jiang, G. Jian, H. Tao, L. Yu, X. Wang, X. Wang, J. Zhu, Z. Hu and Y. Chen, *Energy Environ. Sci.*, 2009, **2**, 224.
35 C. Duarte-Guevara, F.-L. Lai, C.-W. Cheng, B. Reddy, E. Salm, V. Swaminathan, Y.-K. Tsui, H. C. Tuan, A. Kalnitsky, Y.-S. Liu and R. Bashir, *Anal. Chem.*, 2014, **86**, 8359–8367.
36 X. Duan, Y. Li, N. K. Rajan, D. a. Routenberg, Y. Modis and M. a. Reed, *Nat. Nanotechnol.*, 2012, **7**, 401–407.
37 S. J. Slattery, J. K. Blaho, J. Lehnes and K. a. Goldsby, *Coord. Chem. Rev.*, 1998, **174**, 391–416.
38 A. Fog and R. P. Buck, *Sens. Actuators*, 1984, **5**, 137–146.
39 L. Nyholm, *Analyst*, 2005, **130**, 599.
40 D. E. Tallman, C. Vang, G. G. Wallace and G. P. Bierwagen, *J. Electrochem. Soc.*, 2002, **149**, C173.
41 Y. Nishi, T. Sonehara, A. Hokazono, S. Kawanaka, S. Inaba and A. Kinoshita, in *Proceedings of 2010 International Symposium on VLSI Technology, System and Application, IEEE*, 2010, vol. **15**, pp. 120–121.
42 B. Imbert, R. Pantel, S. Zoll, M. Gregoire, R. Beneyton, S. Del Medico and O. Thomas, *Microelectron. Eng.*, 2010, **87**, 245–248.
43 E. De Giglio, M. Guascito, L. Sabbatini and G. Zambonin, *Biomaterials*, 2001, **22**, 2609–2616.
44 Y. Liu, Z. Liu, N. Lu, E. Preiss, S. Poyraz, M. J. Kim and X. Zhang, *Chem. Commun.*, 2012, **48**, 2621–2623.
45 W.-Y. Chung, C.-H. Yang, D. G. Pijanowska, a. Krzyskow and W. Torbicz, *Electron. Lett.*, 2004, **40**, 1115.
46 E. Salm, C. Duarte-Guevara, P. Dak, B. R. Dorvel, B. Reddy, M. A. Alam and R. Bashir, *Proc. Natl. Acad. Sci. U. S. A.*, 2013, **110**, 3310–3315.